AD-A138 834 CONTACT-STRESS ANALYSIS OF ELASTIC-VISCOELASTIC INTERFACE CONDITIONS(U) GARRETT TURBINE ENGINE CO PHOENIX AZ J R SMYTH JAN 84 21-4140(2) 1/1

UNCLASSIFIED N00014-80-C-0870 F/G 11/2 NL

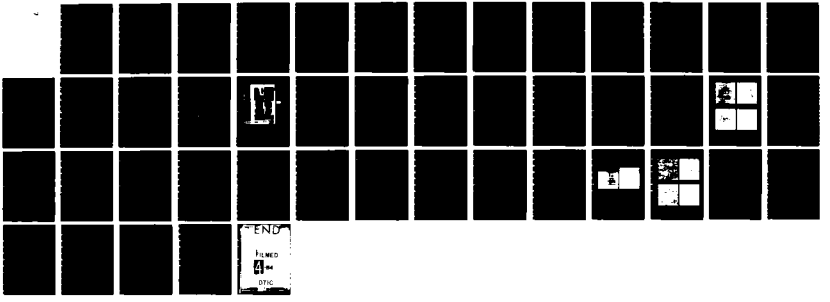

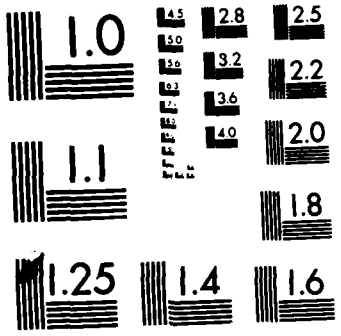

(12)

Report 21-4140(2)
Contract N00014-80-C-0870

CONTACT-STRESS ANALYSIS OF ELASTIC-VISCOELASTIC INTERFACE CONDITIONS

J.R. Smyth

GARRETT TURBINE ENGINE COMPANY
A Division of the Garrett Corporation
111 South 34th Street, P.O. Box 5217
Phoenix, Arizona 85010

January 1984

Final Technical Report
for the Period October 1980 to November 1983

Prepared for

OFFICE OF NAVAL RESEARCH
Department of the Navy
800 North Quincy Street
Arlington, Virginia 22217

UNCLASSIFIED

SECURITY CLASSIFICATION OF THIS PAGE (When Data Entered)

REPORT DOCUMENTATION PAGE		READ INSTRUCTIONS BEFORE COMPLETING FORM
1. REPORT NUMBER	2. GOVT ACCESSION NO. AD-A138834	3. RECIPIENT'S CATALOG NUMBER
4. TITLE (and Subtitle) CONTACT-STRESS ANALYSIS OF ELASTIC-VISCOELASTIC INTERFACE CONDITIONS		5. TYPE OF REPORT & PERIOD COVERED Final Report Oct 80 to Nov 83
		6. PERFORMING ORG. REPORT NUMBER 21-4140(2)
7. AUTHOR(s) J. R. Smyth		8. CONTRACT OR GRANT NUMBER(s) N00014-80-C-0870
9. PERFORMING ORGANIZATION NAME AND ADDRESS Garrett Turbine Engine Company 111 S. 34 St, P.O. Box 5217 Phoenix, AZ 85010		10. PROGRAM ELEMENT, PROJECT, TASK AREA & WORK UNIT NUMBERS
11. CONTROLLING OFFICE NAME AND ADDRESS Office of Naval Research 800 N. Quincy St Arlington, VA 22217		12. REPORT DATE Jan 1984
		13. NUMBER OF PAGES 43
14. MONITORING AGENCY NAME & ADDRESS (if different from Controlling Office)		15. SECURITY CLASS. (of this report) Unclassified
		15a. DECLASSIFICATION/DOWNGRADING SCHEDULE

16. DISTRIBUTION STATEMENT (of this Report)

Reproduction in whole or in part is permitted for any purpose by the United States government.

17. DISTRIBUTION STATEMENT (of the abstract entered in Block 20, if different from Report)

18. SUPPLEMENTARY NOTES

19. KEY WORDS (Continue on reverse side if necessary and identify by block number)

Contact Stress
Elastic-Viscoelastic Interface
High-Temperature Contact Testing

20. ABSTRACT (Continue on reverse side if necessary and identify by block number)

The sliding contact (frictional) behavior of sintered alpha silicon carbide (SASC) was studied over the range of room temperature to 1400°C. The results strongly indicate that a non-elastic mechanism, probably a viscous mechanism, is contributing to the contact behavior of SASC at elevated temperatures. In addition, zirconia, which does not form a viscous layer, was studied for comparison purposes.

DD FORM 1 JAN 73 1473 EDITION OF 1 NOV 65 IS OBSOLETE

UNCLASSIFIED

SECURITY CLASSIFICATION OF THIS PAGE (When Data Entered)

PREFACE

This final technical report is submitted by the Garrett Turbine Engine Company (GTEC), a Division of the Garrett Corporation, under Contract Number N00014-80-C-0870. The effort was sponsored by the Office of Naval Research, Arlington, Virginia, with Dr. R. Pohanka as Contract Monitor.

The following GTEC personnel contributed to the program:

Program Manager	- K.P. Johnson, Propulsion Advanced Technology
Principal Investigator	- J.R. Smyth, Advanced Materials
Technical Advisor	- D.W. Richerson, Advanced Materials
Technical Support	- W.A. Huddleston, Advanced Materials

TABLE OF CONTENTS

CONTACT-STRESS ANALYSIS OF ELASTIC-VISCOELASTIC INTERFACE CONDITIONS FINAL TECHNICAL REPORT

1.0 SUMMARY

This report covers the final phase of a 2-year effort to investigate high-temperature contact-stress behavior of ceramics. This study was an extension of the previous 3-year Contact-Stress Analysis of Ceramic-to-Metal Interfaces Program that concentrated on room-temperature contact-stress behavior.

The overall objective of this total 5-year effort was to systematically study contact interface phenomena, both analytically and experimentally. During the first 4 years of the program, the following activities were accomplished:

- Developed and experimentally verified an analytical model for determining elastic sliding contact stress at room temperatures
- Evaluated the effects of compliant layers, vibrational loads, sliding rates, temperature, and contact geometry on contact stress
- Determined the contact-stress behavior of hot-pressed Si_3N_4, reaction-bonded Si_3N_4, and Sintered Alpha SiC (SASC).

The objective of the final year's effort was two-fold:(1) to develop an understanding of the contact-stress behavior of SASC up to 1400°C and (2) to evaluate the behavior of zirconia (ZrO_2), a non-oxidizing (no viscous layer) material at the same conditions for comparison with SASC in an effort to segregate the elastic and viscous effects on contact behavior. It was

concluded from this study that a viscous mechanism contributed to the elevated-temperature contact behavior of SASC, resulting in high friction compared to a non-oxidizing material (i.e., ZrO_2). The analytical model developed for elastic behavior would require modification to include the viscous effects for predicting the contact-stress behavior of ceramics that oxidize at elevated temperatures.

2.0 BACKGROUND

In the past, design methods and procedures for gas turbine engine components have been based on the use of ductile materials such as metals. However, in recent years numerous programs have focused on employing ceramics for high-temperature gas turbine engine components.

Because of their brittle nature, ceramic components have unique design problems that require modified analytical techniques. Contact stress in ceramic-to-ceramic and ceramic-to-metal interfaces is one example of these problem areas. High, localized stresses in contact regions do not redistribute in ceramics as they do in metals.

The Contact-Stress Analysis of Ceramic-to-Metal Interfaces Program was initiated under Office of Naval Research (ONR) funding in 1978 to systematically study contact interface phenomena. This program included both analysis and specimen testing and evolved into the present effort in 1980.

Since that time, proposals were prepared and contract modifications were awarded to increase the program scope, budget, and period of performance on an annual basis. Thus, each year's efforts have been detailed in separate documents.[1-4*] Although a brief review of these efforts is presented herein, the major portion of this report is a summary of the most recent activity, covering the work performed from February 1983 to November 1983.

*A list of references is presented in Section 7.0.

2.1 Room-Temperature Contact Testing and Analysis

The emphasis during the first year of this program centered on the use of finite-element computer techniques, including zoom modeling, to effectively calculate the complex state of stress in a contact interface zone without compliant media. Frictional forces were identified as the key to understanding contact behavior at ceramic interfaces.[1]

Work during the second year of the program focused on compliant media at the interface. The beneficial load-redistribution characteristics of compliant media were demonstrated through specimen testing and analysis using a finite-element approach. Specimen testing was also used to evaluate the effects of surface finish, machining direction, surface treatments, and compliant media durability. Over the load range examined in this program at room temperature, soft compliant layers such as platinum and fiber metals demonstrated more durability than materials with less compliance.[2]

The third year of the program involved the effect of vibrational stresses on contact-surface failures. The stresses in this region are due to a complex interaction between contact and dynamic (vibrational) stresses. It was shown that, as the contact loads increased, there was a corresponding decrease in the dynamic stress level at which failure occurred. It was concluded that the stresses due to contact forces combine with dynamic stresses to yield higher resultant stresses, causing the ceramic component to fail. The detrimental effect of contact loading decreased with decreasing contact force. It was also found that the use of compliant layers effectively decreased the detrimental effects of contact forces.[3]

Contact testing through the third year of the program had been conducted at room temperature. The ONR contact-stress program had achieved the development and verification of

finite-element analysis for localized contact-stress distributions and had substantially increased the general level of understanding the effects of biaxial loading on fracture probability. However, parallel studies under the DARPA/Navy Ceramic Engine Demonstration Program[5,6] and the NASA/DOE Advanced Gas Turbine Program[7] indicated that contact-stress mechanisms were different at elevated temperatures for some ceramic materials, and that the finite-element analysis model developed under the ONR program would require modification for use at these high-temperature conditions. Paragraph 2.2 describes the results of high-temperature contact-stress testing during the fourth year of the program.

2.2 High-Temperature Contact Testing and Analysis

The fourth year of the program dealt with the effects of temperature on the contact behavior of SASC. Studies conducted over the range of room temperature to 1100°C showed that the nature of the friction curves was significantly different at elevated temperatures.

Figure 1 shows typical force/time curves for SASC at four different temperatures. There is no clear delineation between static and dynamic behavior at temperatures of 600°C and below. At 900° and 1100°C, there is a distinct breakaway that defines the static coefficient of friction. The recovery force (F_R) increases with increasing temperature. This force is a measure of the relaxation in the tangential force that takes place after the crosshead of the testing machine is stopped at the end of a dynamic test. The specimens move relative to each other, relieving the tangential force.

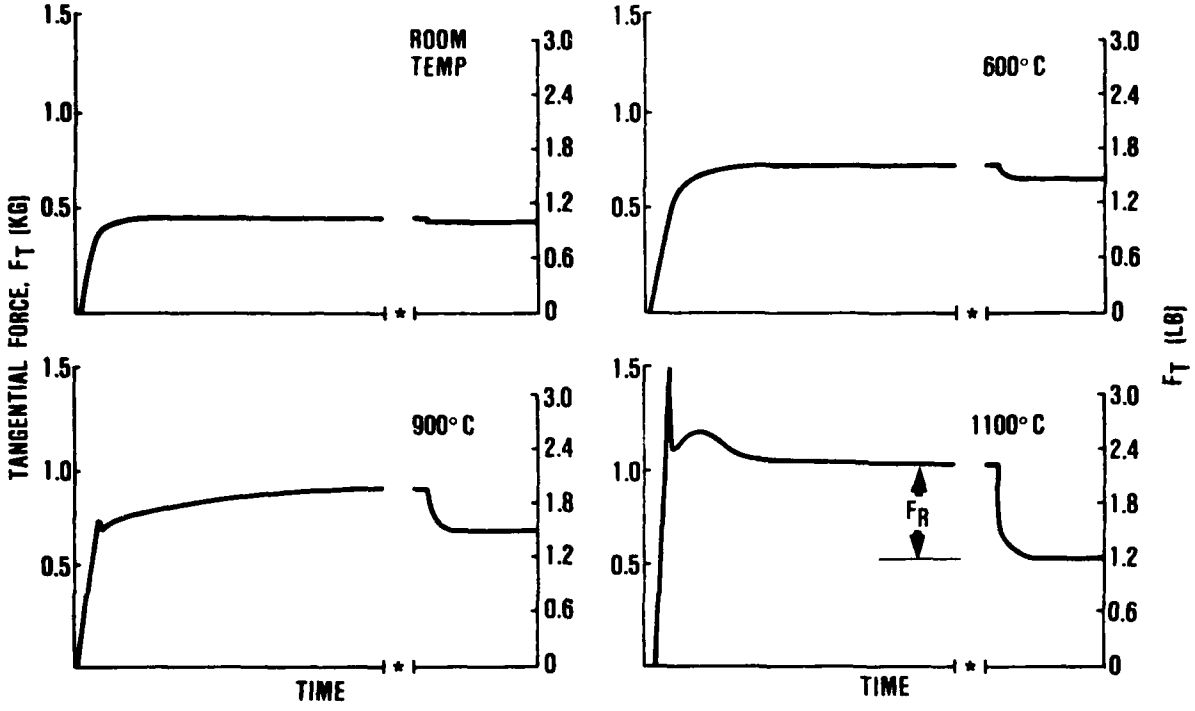

Figure 1. Force/Time Curves for a 1.4 kg Normal Force.

The static frictional force as a function of temperature is presented in Figure 2. The static force increases slightly with temperature up to 900°C for each of the normal forces tested. Above 900°C, there is a dramatic increase in the static force for normal forces of 1.4 and 2.7 kg, while specimens under the 4.5-kg normal force do not exhibit this behavior. The 0.5-kg normal force situation shows a continuous increase in static force with temperature, starting at approximately 600°C. If the contact behavior were purely elastic, there would be no increase in frictional force with increased temperature over the temperature range of interest. Therefore, these results suggest that some nonelastic mechanism is contributing to the measured frictional force.

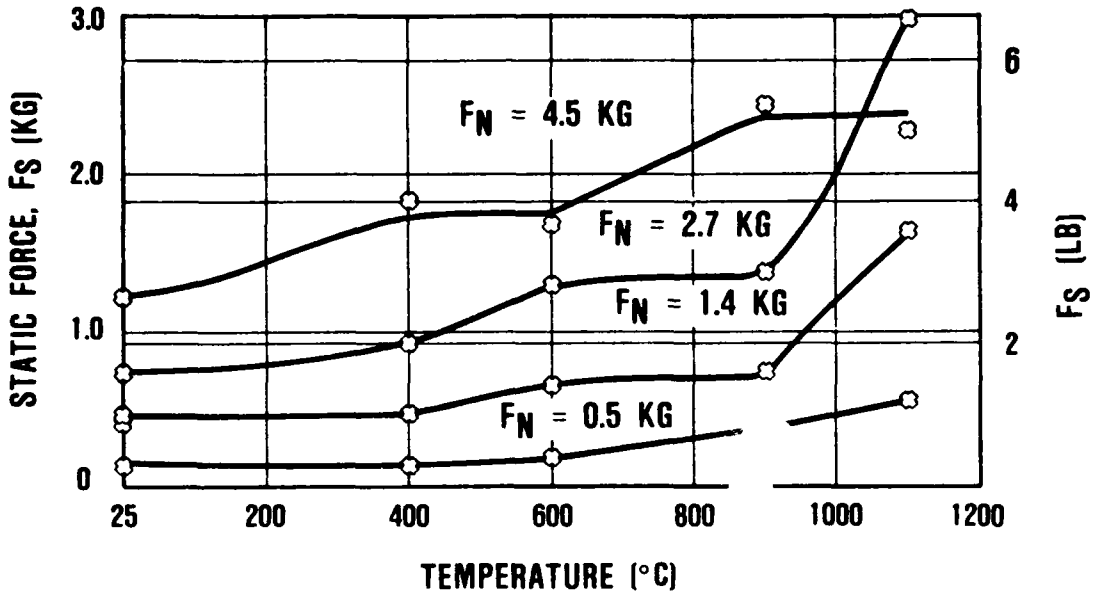

Figure 2. Static Frictional Force as a Function of Temperature (Line Contact, 0.05 cm/min Sliding Rate).

In terms of coefficient of static friction, there is a four-fold increase from room temperature to 1100°C for normal forces below 4.5 kg. The elastic model for contact stress shows that tensile stress at the contact interface strongly depends on the coefficient of friction. Using the measured coefficients of static friction at 1100°C and the elastic model computer program developed in Reference 1, the predicted peak tensile stress for normal forces of 0.5 to 4.5 kg ranges from 408 to 990 MPa, respectively. These values exceed the baseline material strength (278 to 368 MPa) and should result in considerable surface damage and strength reduction if a purely elastic model pertains. However, the measured strengths of the specimens after contact testing show no measurable strength reduction. This provides further evidence that the high-temperature contact conditions are not purely elastic and that the previously developed elastic model requires modification to include nonelastic effects.

A large time-dependent recovery force was observed, and experimental results showed that the sliding friction at elevated temperatures is a function of both contact area and the nature of the glassy surface layer. These two factors strongly indicate that a viscous and/or viscoelastic mechanism is contributing to the contact behavior of SASC. It was also concluded that additional elevated-temperature experimental data is needed to understand contact behavior and to provide input for developing an analytical model that addresses non-elastic behavior at elevated temperatures.[4,8]

3.0 EXPERIMENTAL PROGRAM CONDITIONS

The current experimental program was designed to produce data that would allow segregation of elastic, viscous, and other effects and provide numerical inputs to support development of analytical models for predicting the magnitude of contact damage at elevated temperatures.

For this study, SASC test specimens were evaluated in line contact up to 1400°C. The normal forces applied were 0.5, 1.4, 2.7, and 4.5 kg. Contact behavior was investigated at sliding rates of 0.05 and 0.005 cm/min.

The effect of surface pre-treatment was also evaluated. The pre-treatment consisted of either lapping the surface or oxidizing the surface before testing. As reported previously,[3] at the lower normal forces used in this study, there was no measurable contact-stress effect on the retained strength of SASC. Therefore, SASC strength after contact testing was not determined in this year's effort.

Cubic stabilized zirconia (CSZ) test specimens were evaluated in line contact over the range of room temperature to 1400°C. The normal forces applied were 0.5, 1.4, 2.7, and 4.5 kg, and the sliding rate was 0.05 cm/min. Zirconia does not oxidize at elevated temperatures and is not likely to have a viscous surface. Therefore, it was used as a control material for comparison with SASC in an effort to segregate elastic and viscous effects on friction and interface stresses. Specimens were fractured in four-point bending after contact testing to determine if the contact loads caused a reduction in strength.

Approximately 120 individual sliding contact tests were performed on SASC and CSZ specimens. The contact surfaces were examined by optical microscopy (40X) and scanning electron microscopy (SEM) after testing.

The program was originally planned to include a task to test a partially stabilized zirconia (PSZ), which has higher fracture strength and toughness than CSZ, in order to obtain data comparing the effects of toughness on the contact-damage sensitivity of a ceramic material. However, the CSZ did not sustain any contact damage at the low normal forces (4.5 kg and less) employed in this study. Also, under a parallel program[9] to evaluate in detail the contact behavior of various PSZ materials, it was determined that these materials do not sustain contact damage until normal forces exceed 11 kg. Therefore, the decision was made to concentrate manpower and program funds on efforts to improve the understanding of the frictional behavior of SASC, as reported in Section 4.0.

4.0 ELEVATED-TEMPERATURE CONTACT TEST APPARATUS AND PROCEDURE

Figure 3 is a schematic of the contact test apparatus. The furnace is lined with high-temperature fiber insulation, can be heated rapidly, and has a capability in excess of 1400°C. The clam-shell construction and swivel mounting allow the furnace to be moved out of the way for specimen alignment and calibration. Figure 4 is a photograph of the test apparatus with the furnace opened to show placement of the test specimens.

To improve alignment and eliminate excess movement of the test specimen in the test fixture and test apparatus, the specimens are machined to very close tolerances, as shown in Figure 5. Specimen B is held stationary during the test, and its 0.32-cm radius surface is held in contact with Specimen A. Specimen A is moved tangentially during the test, and its 0.64-cm flat surface is used as the test surface.

Each experiment consisted of the following procedure. The specimens were placed in the test fixture not contacting each other. The furnace was closed around the test apparatus and heated to the desired temperature in approximately 15 to 20 minutes. When the furnace equilibrated at the test temperature, the normal force was applied. The specimens were held in contact by the normal force for a specified time. Relative motion was then induced by the testing machine(product of the Instron Corp., Canton, MA), and the tangential force was measured by the load cell. The sliding distance (contact distance) for each test was 0.076 to 0.15 cm. The data obtained is in the form of a force/time curve, from which static, dynamic, and recovery forces could be determined. These measured forces were used to analyze the contact behavior.

After each test, the specimens were cooled to room temperature and examined visually (40X). Selected specimens were also examined by scanning electron microscopy.

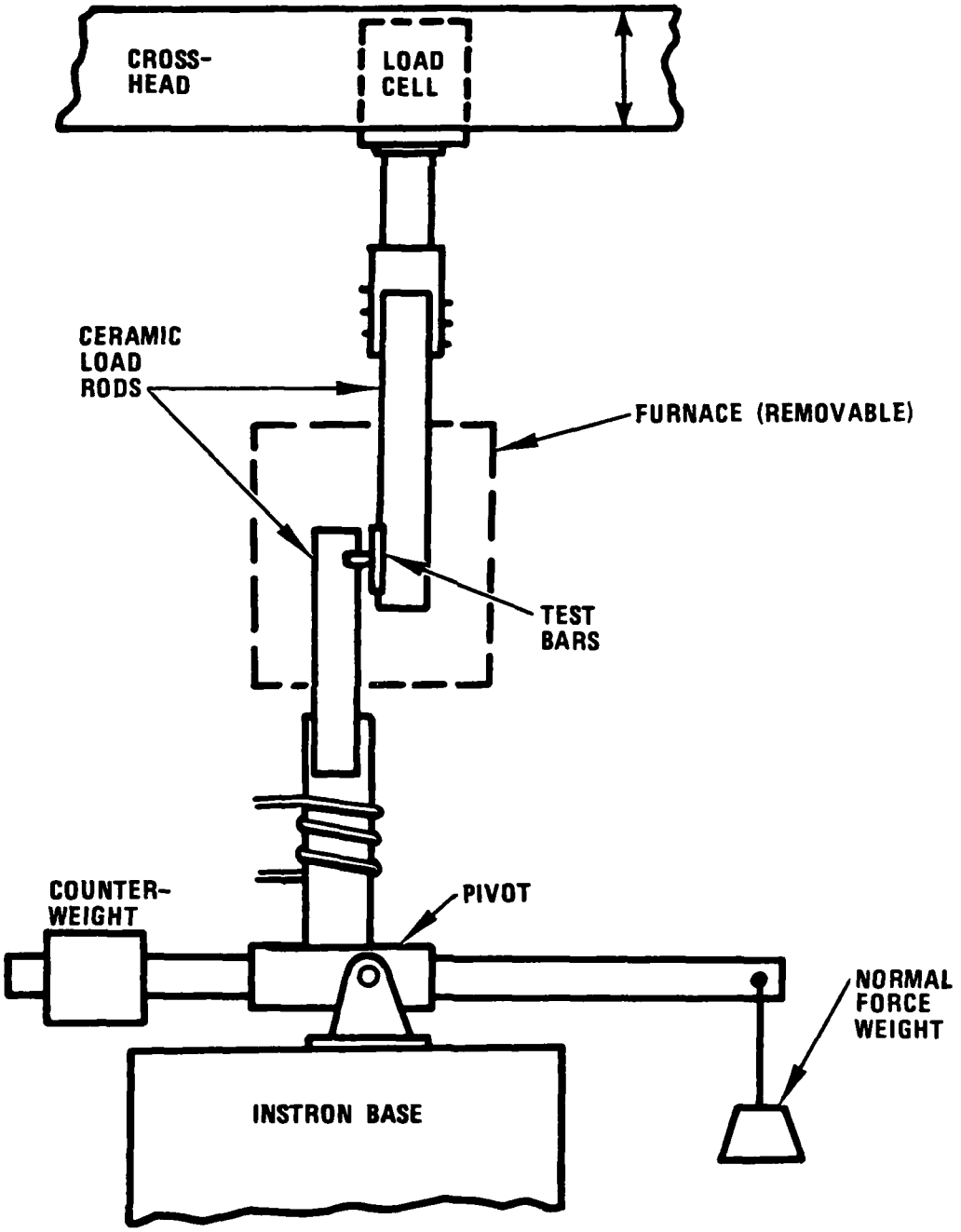

Figure 3. Design of Contact-Stress Rig.

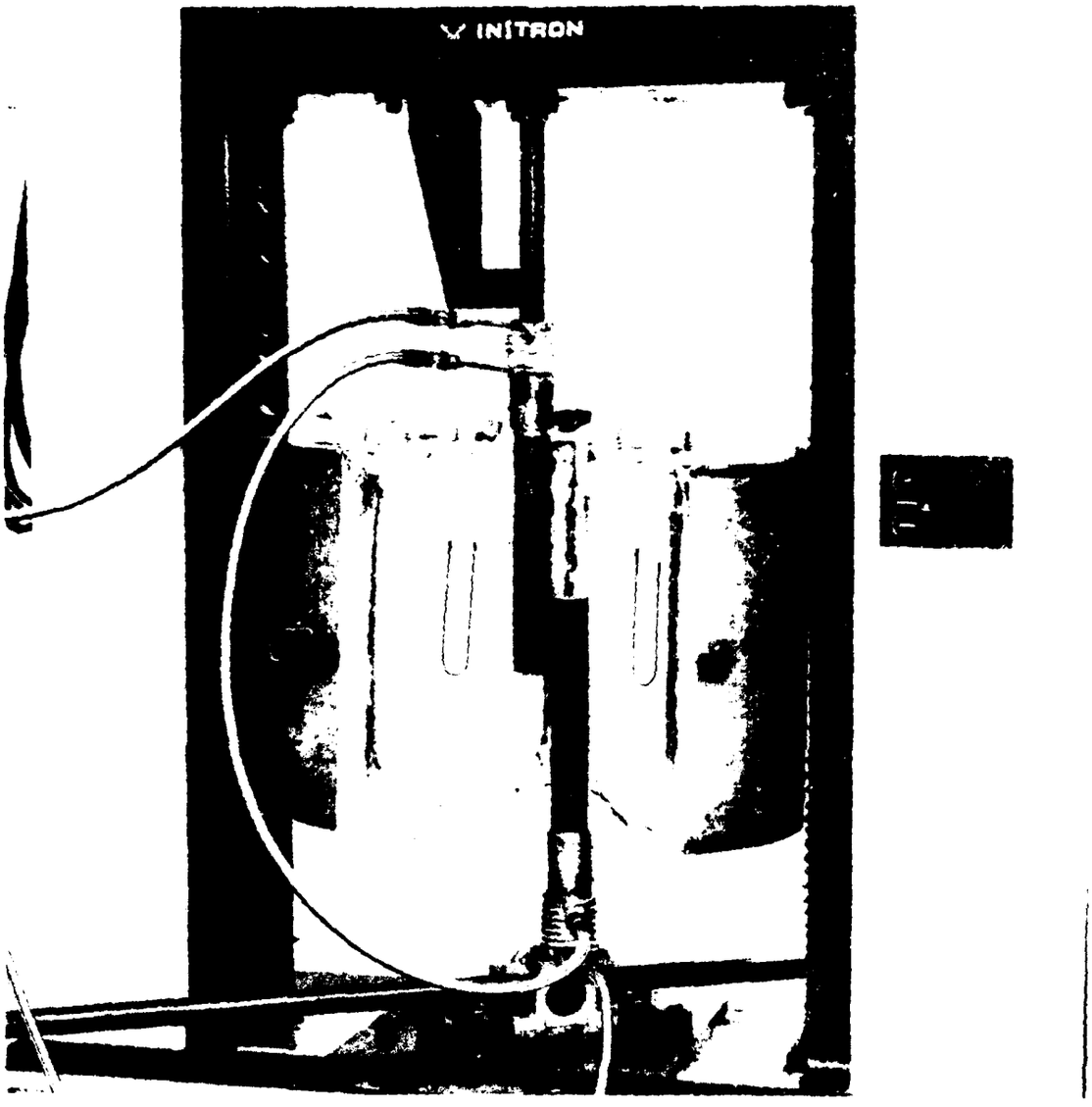

Figure 4. Contact-Stress Rig.

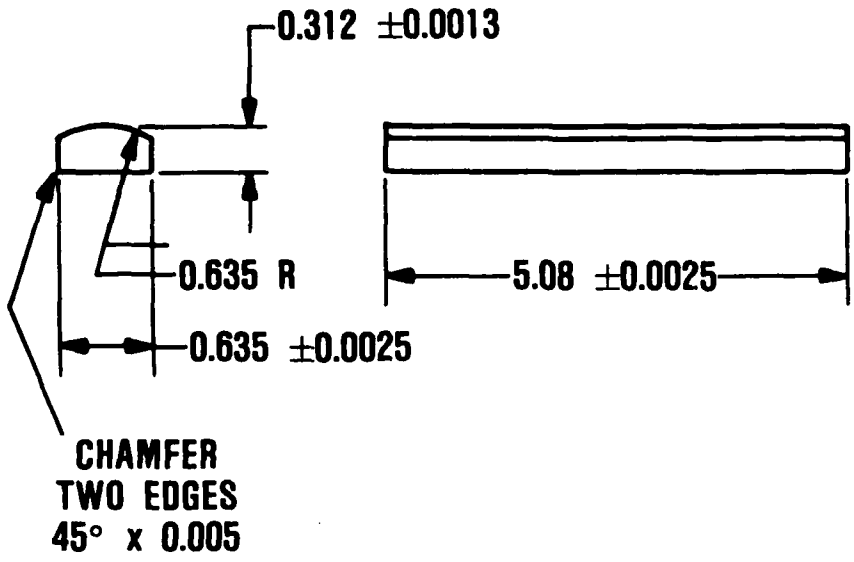

SPECIMEN A

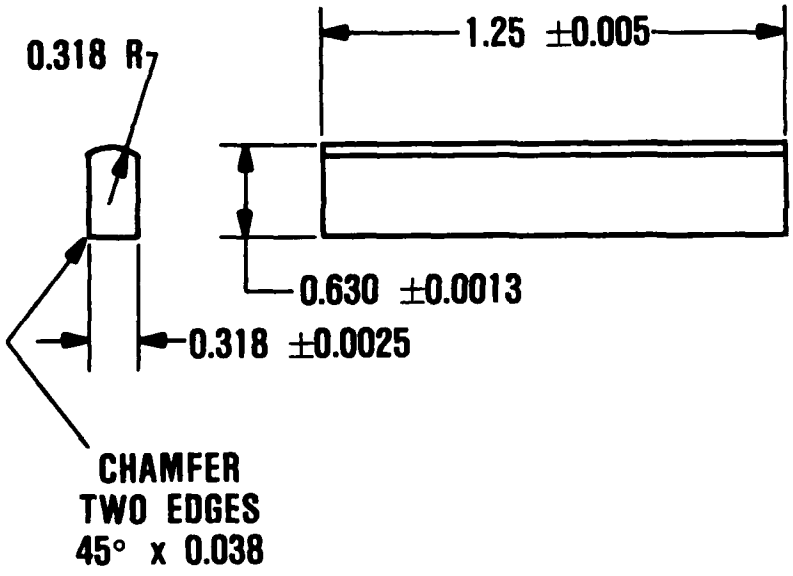

SPECIMEN B

DIMENSIONS, CM

Figure 5. Contact-Stress-Rig Test Bars.

5.0 TEST RESULTS

5.1 Interface Contact Behavior of SASC, Room Temperature to 1400°C

A series of experiments was performed to measure frictional forces at 1200°, 1300°, and 1400°C with applied normal forces of 0.5, 1.4, 2.7, and 4.5 kg. The purpose of these experiments was to further evaluate the high-temperature contact behavior of SASC involving the apparent increase in coefficient of friction with temperature, as reported in 1982.[4]

The coefficient-of-friction results for this series of experiments are presented in Figures 6 through 9. Previously reported data[4] is included for completeness. Within the data variance, a trend emerges in the coefficient of friction as a function of temperature. In general, both the static coefficient of friction (μ_S) and the dynamic coefficient of friction (μ_D) increase with temperature from approximately 900°C to approximately 1300°C and then decrease at higher temperatures. These results are consistent with the hypothesis that a viscous mechanism is contributing to the contact behavior of SASC at elevated temperatures.

If a SiO_2 layer is formed on the surface of the specimen prior to or during testing, it is reasonable to assume that a viscous glassy layer would form over some temperature range (900° to 1300°C). As the temperature increases, the layer would become thicker, creating more resistance (increase in apparent friction) between the sliding specimens. Above some temperature (1300°C), the viscosity of the glassy layer would decrease, thereby reducing the resistance (decrease in apparent friction) between the sliding specimens. Thus, the coefficient

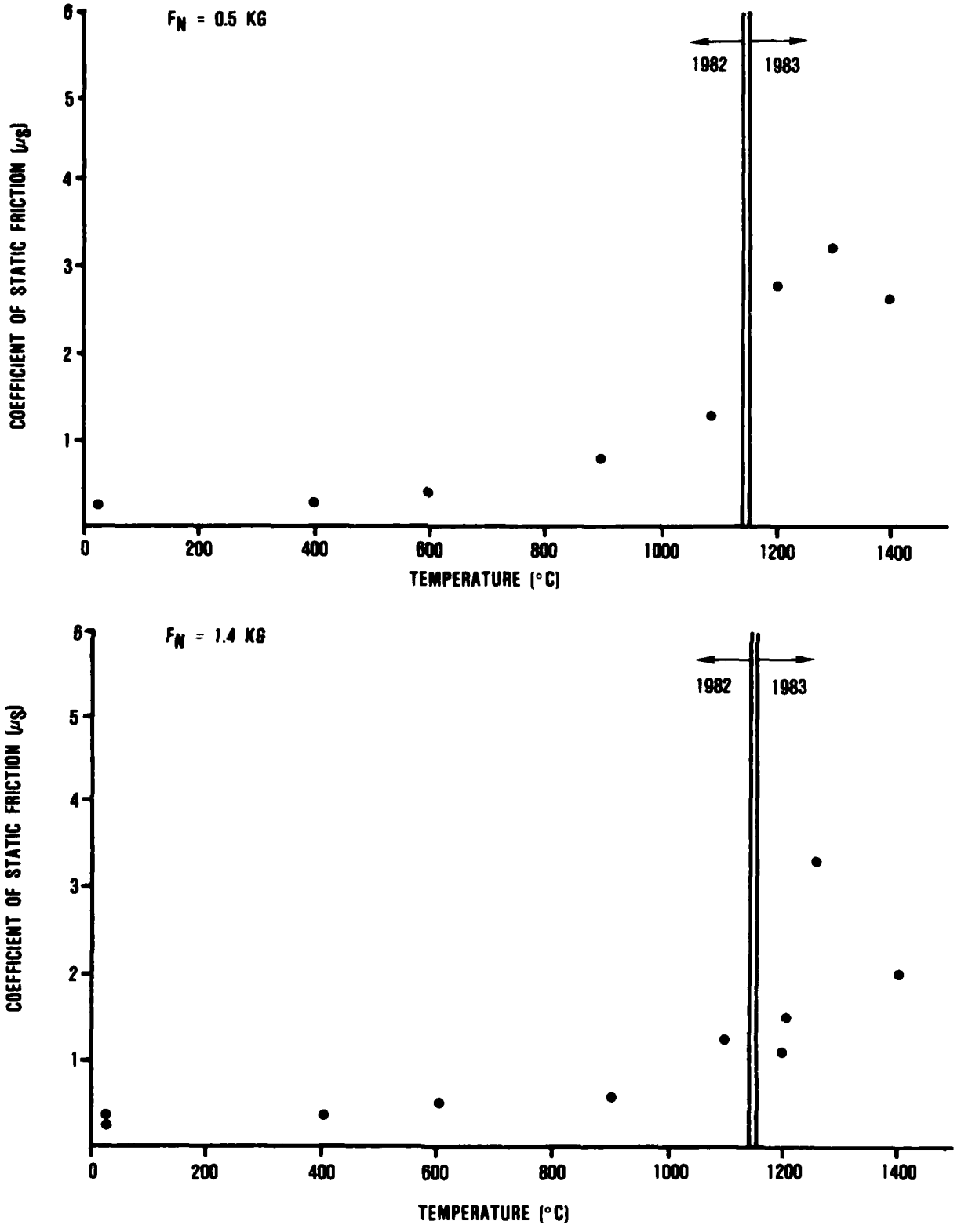

Figure 6. Coefficient of Static Friction as a Function of Temperature for SASC at Normal Forces of 0.5 and 1.4 kg (Line Contact, 0.05 cm/min Sliding Rate).

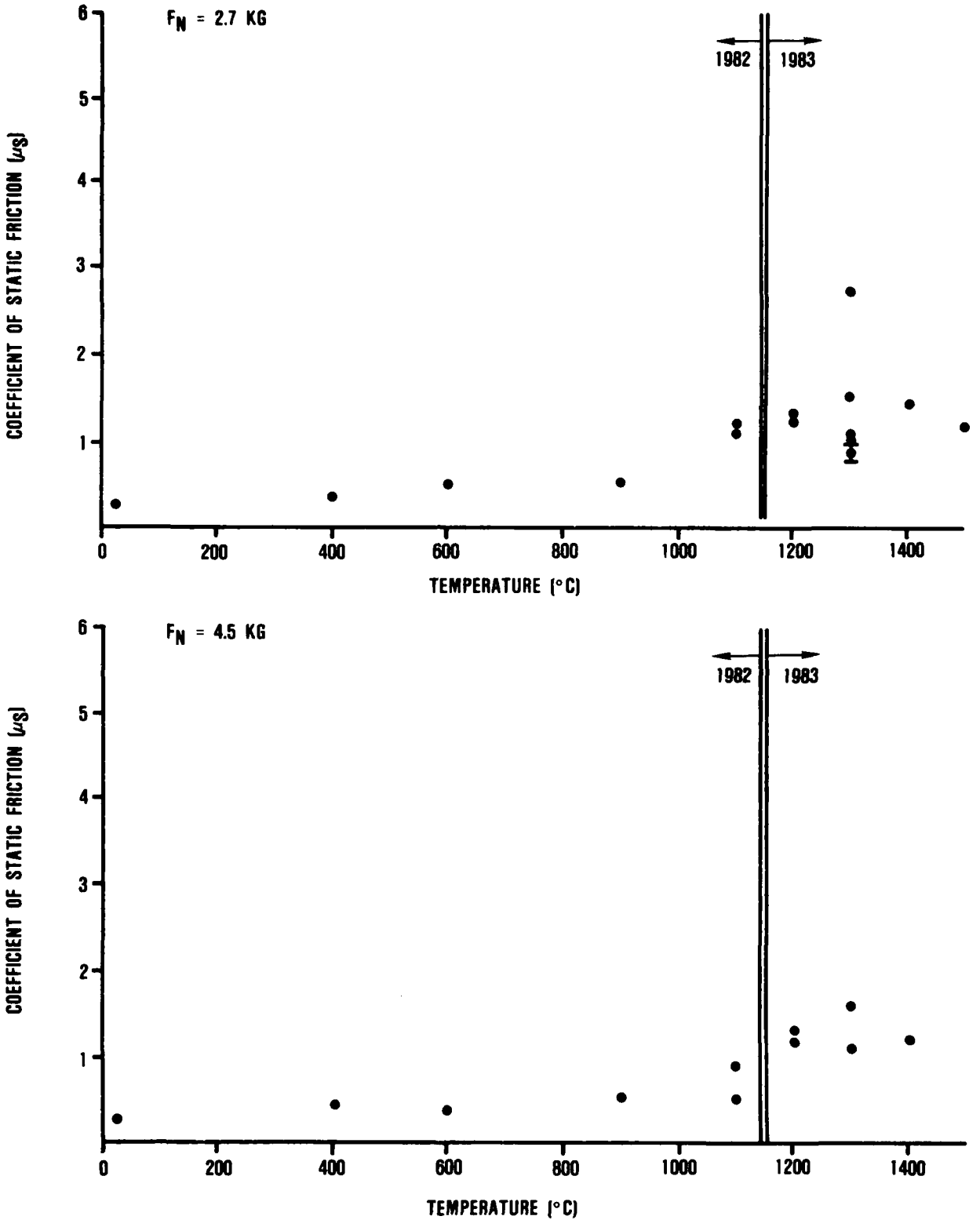

Figure 7. Coefficient of Static Friction as a Function of Temperature for SASC at Normal Forces of 2.7 and 4.5 kg (Line Contact, 0.5 cm/min Sliding Rate).

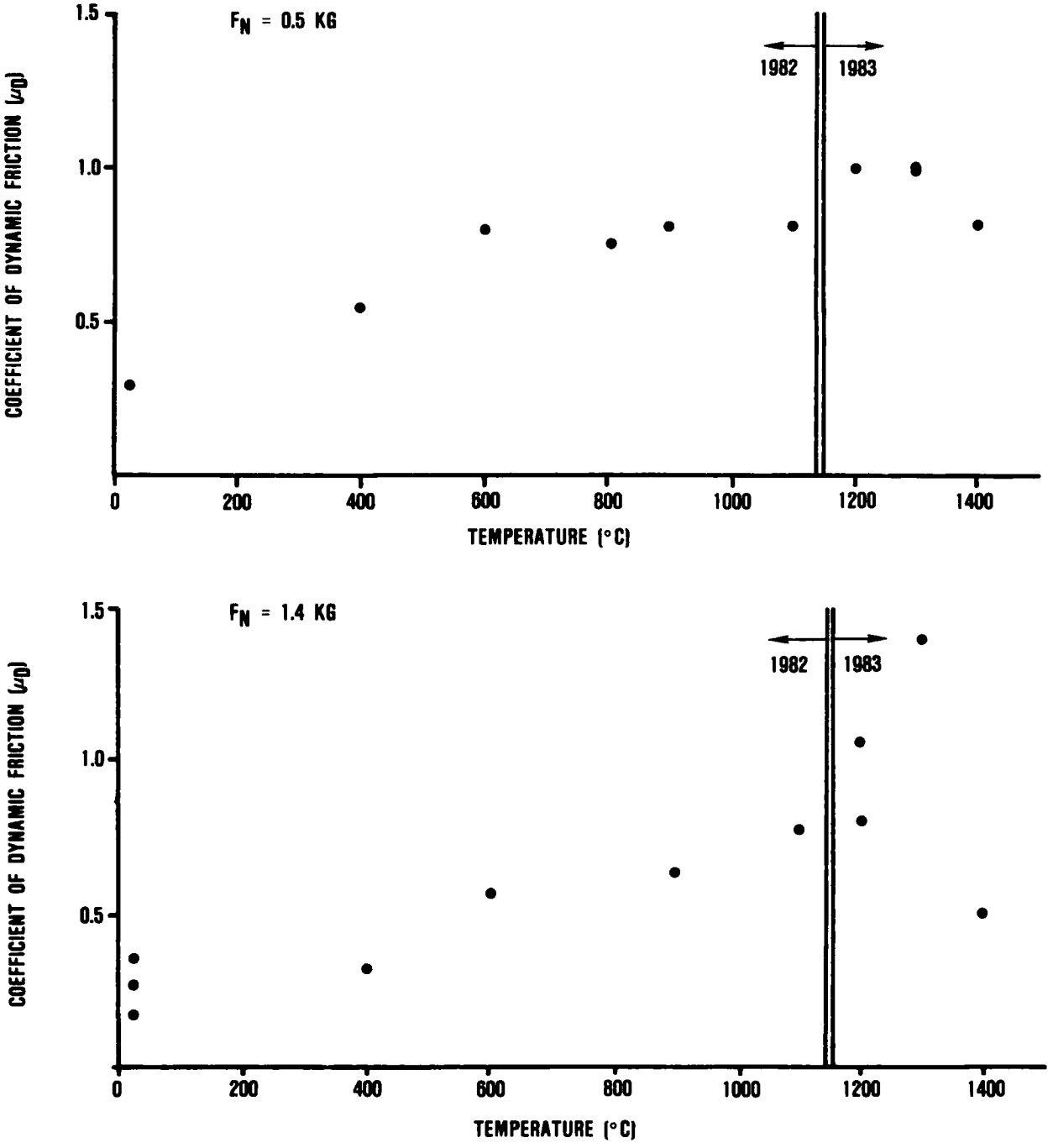

Figure 8. Coefficient of Dynamic Friction as a Function of Temperature for SASC at Normal Forces of 0.5 and 1.4 kg (Line Contact, 0.05 cm/min Sliding Rate).

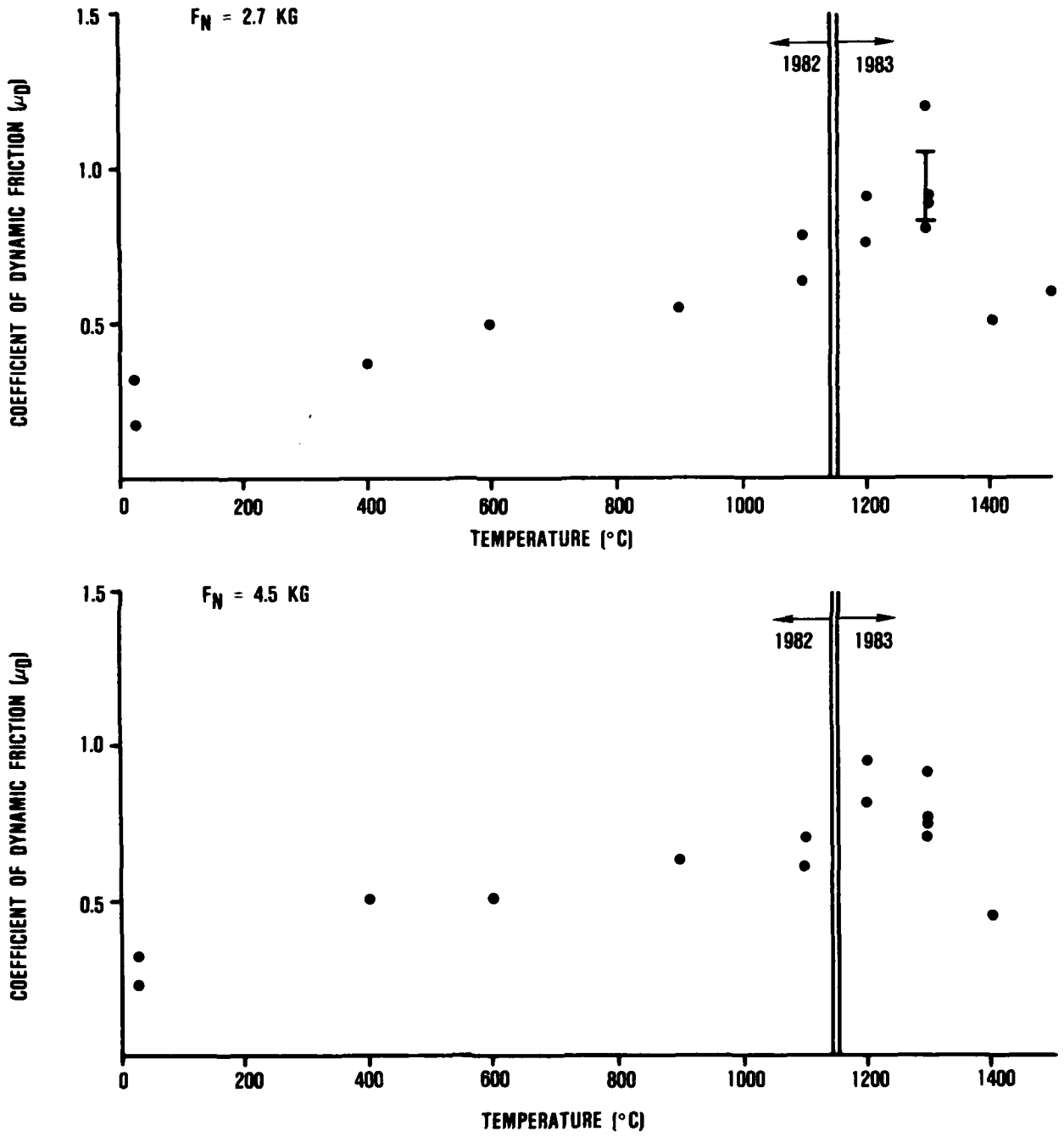

Figure 9. Coefficient of Dynamic Friction as a Function of Temperature for SASC at Normal Forces of 2.7 and 4.5 kg (Line Contact, 0.05 cm/min Sliding Rate).

of friction (μ) of SASC at elevated temperatures appears to be a function of both the thickness (d) and viscosity (η) of the surface layer in the form:

$$\mu \alpha \frac{d}{\eta}$$

The scatter in the data (at 1200° or 1300°C) can be explained if the viscous layer hypothesis is considered. The amount (thickness) of glassy layer formed may vary depending on the pretest surface treatment (as-machined or oxidized) and/or the length of time the specimens are exposed to elevated temperatures during testing. To evaluate this possibility and assure that the scatter is not related to the contact test rig or test procedure, six specimens were evaluated in the as-machined condition. Their μ_S and μ_D were determined at a 2.7 kg normal force and 1300°C. The heating rate and time at temperature were the same in each test. The results of this experiment are shown in Figures 7 and 9 as a range between the two horizontal line segments. These results indicate that the contact test rig and procedure lead to reproducible results.

Figure 10 presents scanning electron photomicrographs of typical contact areas after testing at 1100°, 1200°, 1300°, and 1400°C. As shown in the figure, the extent of glass in the contact area increases with test temperature. At 1100°C, there is no evidence of glass; at 1200°C, glass starts to appear; and at 1400°C, the entire contact surface exhibits a glassy appearance. Also, the amount of debris left on the surface increases with temperature. This would suggest that there is a surface layer whose adhesion decreases with increased temperature. This debris can collect in front of the sliding specimen and could contribute to the measured coefficient of friction.

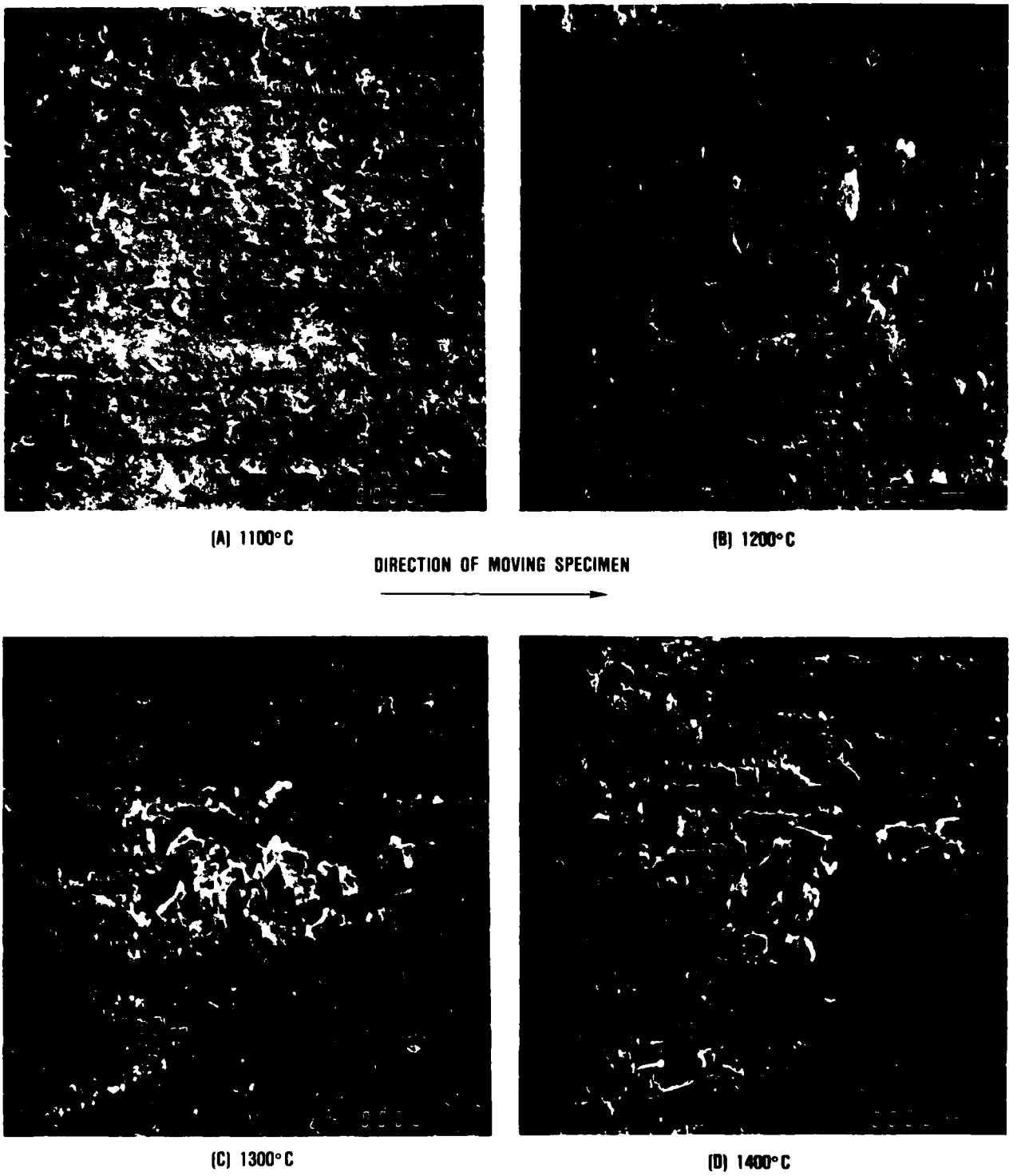

Figure 10. Scanning Electron Photomicrographs of SASC Contact Areas after Testing at Various Temperatures and a 4.5 kg Normal Force.

As reported previously,[4] the recovery force (F_R) appears to be related to the magnitude of the nonelastic contribution to contact behavior. The magnitude of this force is more than can be explained elastically and is time-dependent (Figure 1), suggesting a viscous or viscoelastic behavior. Figure 11 shows the measured F_R for experiments conducted at a 2.7 kg normal force over the range of room temperature to 1400°C. Again, data generated last year is included for completeness. Also included are the six data points obtained from the controlled experiment discussed previously. As with μ_S and μ_D, the F_R increases with temperature between 900° and 1300°C, and decreases at temperatures above 1300°C. Once again, this would be consistent with the viscous layer hypothesis assumming that F_R is a function of the viscosity and amount of glass.

To further evaluate any viscosity (time-dependent) effects that might contribute to the measured coefficient of friction of SASC, several tests were conducted at a slower sliding rate (0.005 cm/min). The hypothesis was that, if there were a time-dependent effect, the measured μ_S and μ_D would vary with the rate of sliding. Tests were conducted over the temperature range of 900° to 1400°C at a 2.7 kg normal force. The results of these experiments are shown in Figure 12 along with the general trend of tests conducted at 0.05 cm/min (for comparison). At the slower sliding rate, the coefficient of friction increases with temperature and then decreases, with the maximum value in the 1100° to 1300°C range. Based on the limited data taken, little more can be concluded.

To further assess the effects of thin surface oxide layers, samples were exposed to preoxidation under two separate conditions: 1204°C for 4 hours and 1204°C for 72 hours. It was assumed that a thicker oxide layer would be present after the longer exposure. These specimens were then contact-tested at 900° and 1400°C with a 2.7 kg normal force.

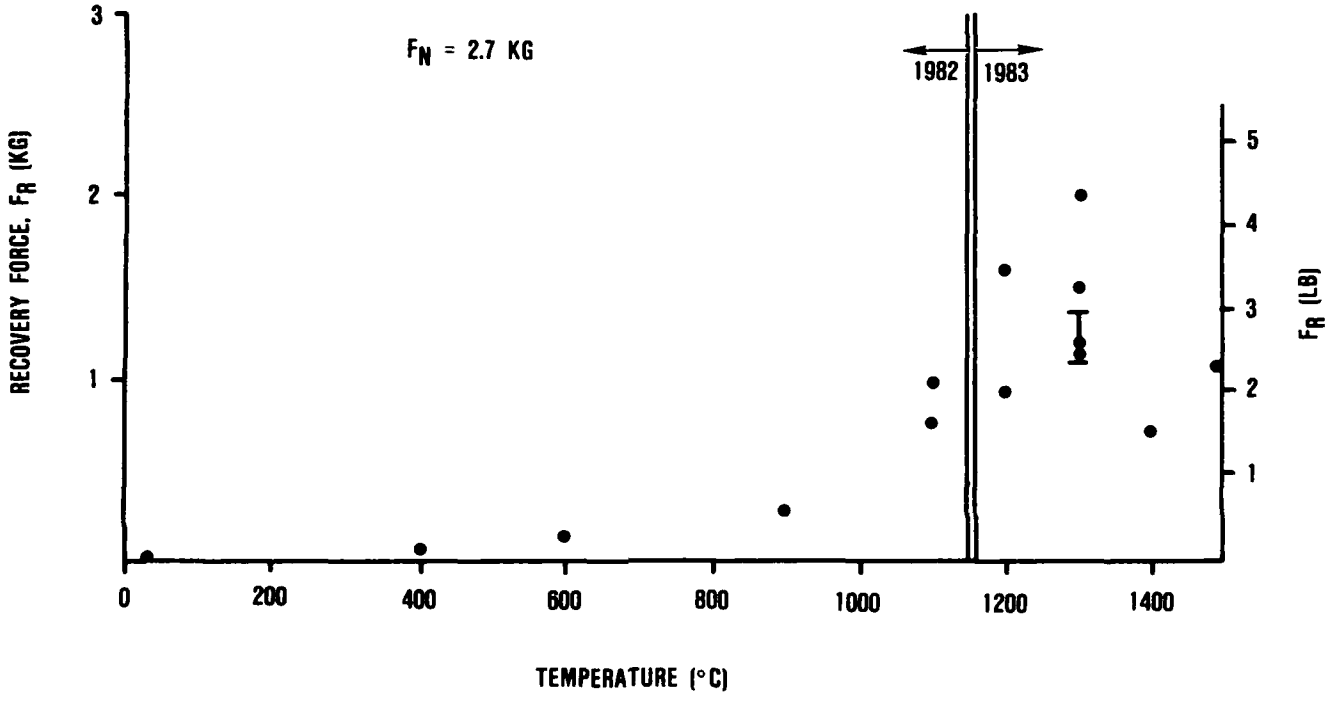

Figure 11. Recovery Force as a Function of Temperature for SASC.

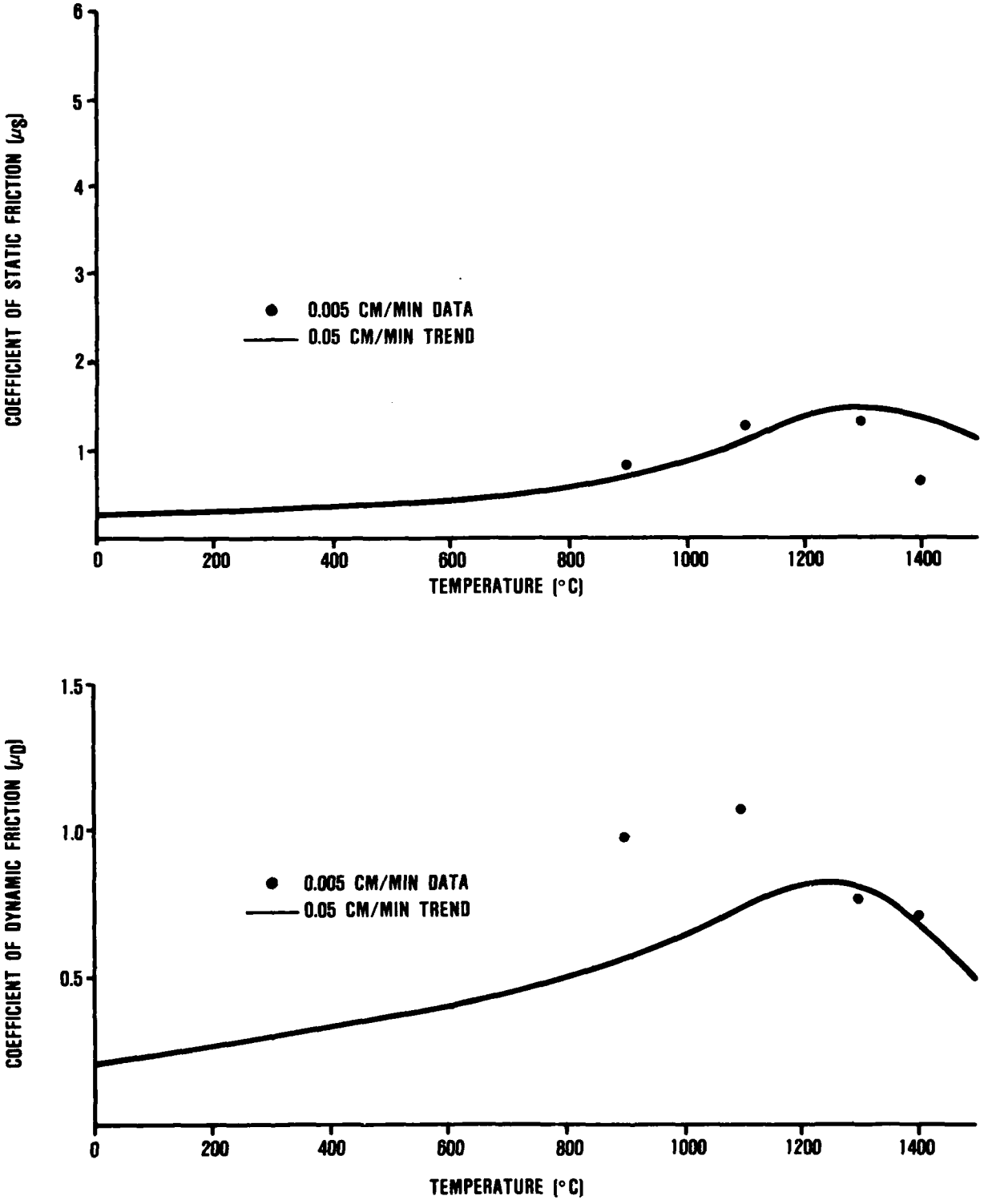

Figure 12. Coefficient of Friction as a Function of Temperature for SASC at 0.005 cm/min Sliding Rate (Line Contact, 2.7 kg Normal Force).

The results of this experiment, presented in Table 1, show no significant difference in μ_D between the specimens oxidized for 4 hours and 72 hours. Although there appears to be a significant difference in μ_S, any conclusions would be premature because of the limited data. The contact areas did not reveal any significant differences after testing and were generally similar to those reported in Figure 10.

TABLE 1. COEFFICIENT OF FRICTION OF SASC OXIDIZED FOR 4 HOURS AND 72 HOURS AT A 2.7 KG NORMAL FORCE.

Temperature (°C)	4-Hour Oxidation		72-Hour Oxidation	
	μ_S	μ_D	μ_S	μ_D
900[1]	0.81 ±0.04	0.73 ±0.02	1.15 ±0.10	0.74 ±0.01
1400[2]	1.26 ±0.06	0.73 ±0.06	0.95 ±0.05	0.76 ±0.05

[1] Average of six tests on same test bar
[2] Average of five tests on same test bar

A third experiment was conducted to evaluate the effect of surface finish (i.e., the area of contact) on the measured coefficient of friction. Several specimens were lapped to a uniform surface flatness of 3 to 5 μm. The specimens were oxidized for 4 hours at 1204°C and then contact-tested at 1300°C and a 2.7 kg normal force. The μ_S and μ_D measured were 1.73 ±0.14* and 1.29 ±0.10*, respectively. These results are higher than those obtained under the same test conditions for as-machined specimens (see Figures 7 and 8). It can be assumed

*Average of six tests on same specimen

that, with a lapped surface, a larger area will be under the contact load. If the frictional behavior of SASC is purely elastic, the coefficient of friction should be independent of contact area. However, in the case of a viscous mechanism, the area of contact would produce an increase in the measured coefficient of friction due to the increased drag of the viscous layer.

5.2 Interface Contact Behavior of CSZ, Room Temperature to 1400°C

CSZ does not oxidize at high temperature and is not likely to have a viscous surface. Therefore, it was used as a control material for comparison with SiC in an effort to segregate elastic and viscous effects on friction and interface stresses.

A series of experiments was conducted using ZDY4 CSZ contact specimens (produced by Coors Procelain Company, Golden, CO). The μ_S, μ_D, and F_R were measured over the range of room temperature to 1400°C for normal forces of 0.5, 1.4, 2.7, and 4.5 kg.

Figure 13 shows typical force/time curves for four different temperatures. There is no clear delineation between static and dynamic behavior at temperatures of 1100°C and below. At 1400°C, there is an indication of a breakaway force that defines μ_S. This behavior is significantly different from the frictional behavior of SASC, where distinct breakaway was observed at temperatures as low as 900°C.

At elevated temperatures, the magnitudes of μ_S and μ_D for SASC were very different. For the CSZ specimens, both coefficients of friction were essentially the same. Figures 14 and 15 present the results of the μ_S measurements. The coefficients of friction for CSZ are low (<0.8) at all temperatures

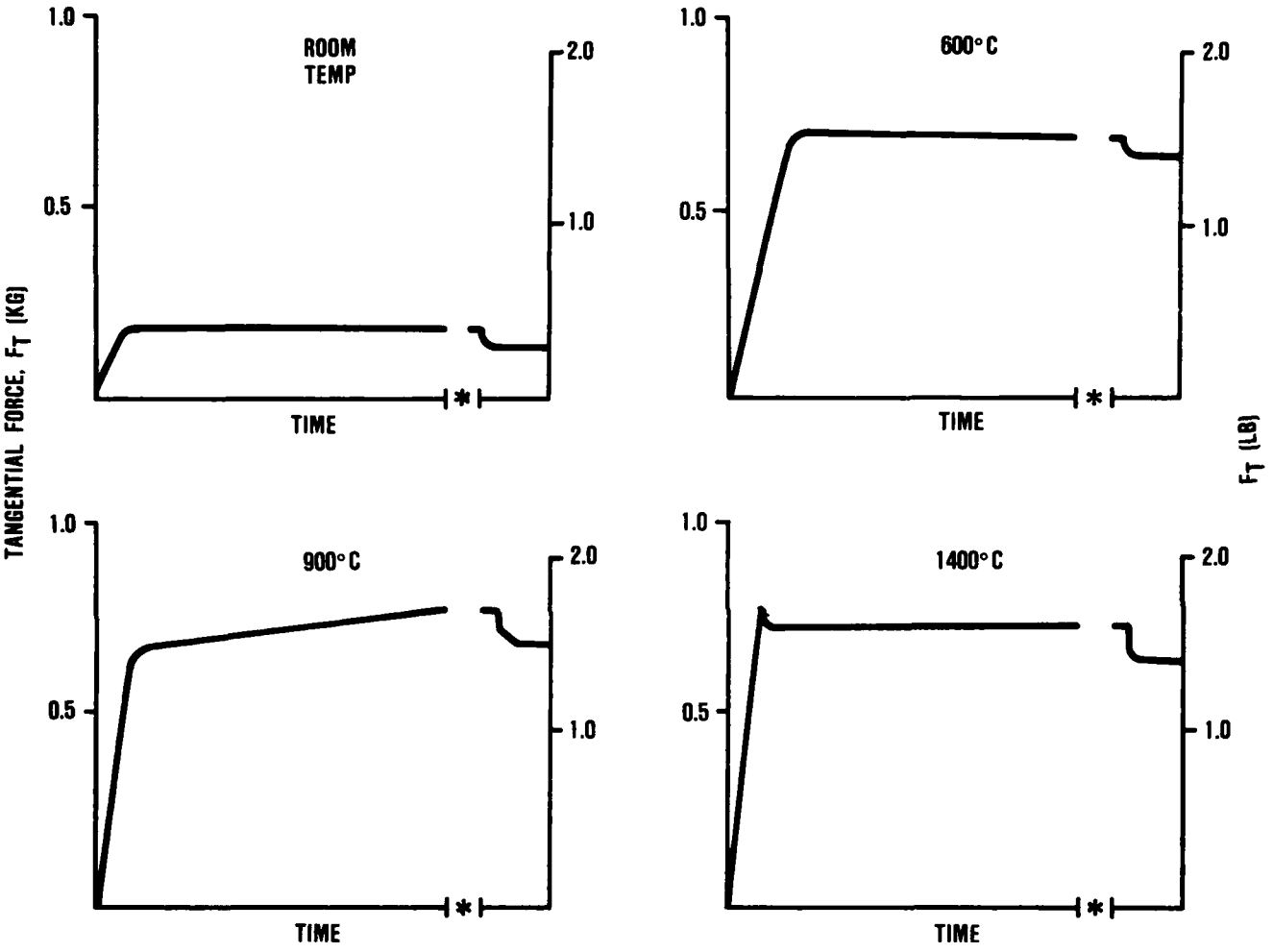

*CROSSHEAD OF TESTING MACHINE STOPPED

Figure 13. Force/Time Curves for ZDY4 CSZ at a 1.4 kg Normal Force.

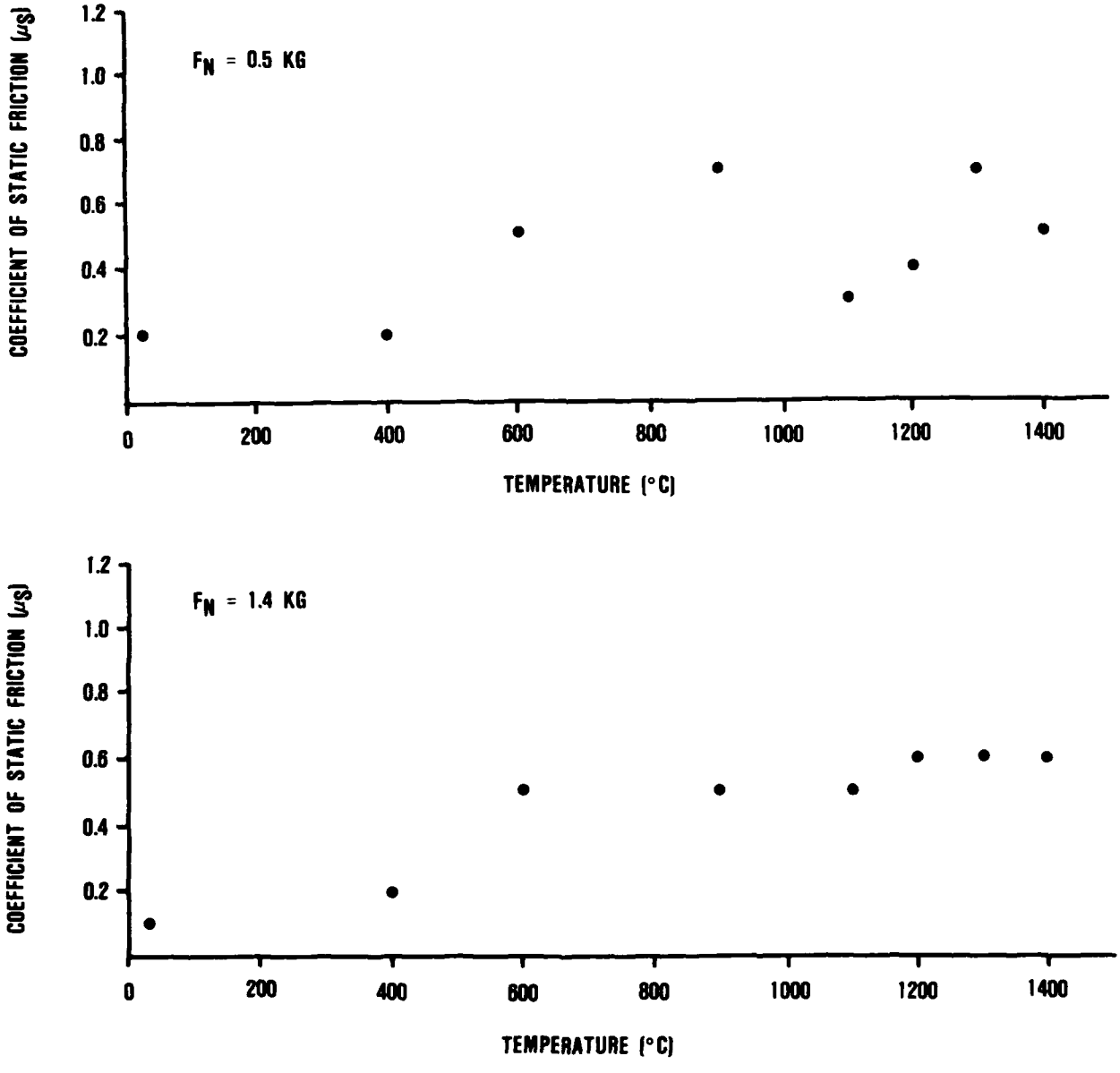

Figure 14. Coefficient of Static Friction as a Function of Temperature for CSZ at Normal Forces of 0.5 and 1.4 kg (Line Contact, 0.05 cm/min Sliding Rate).

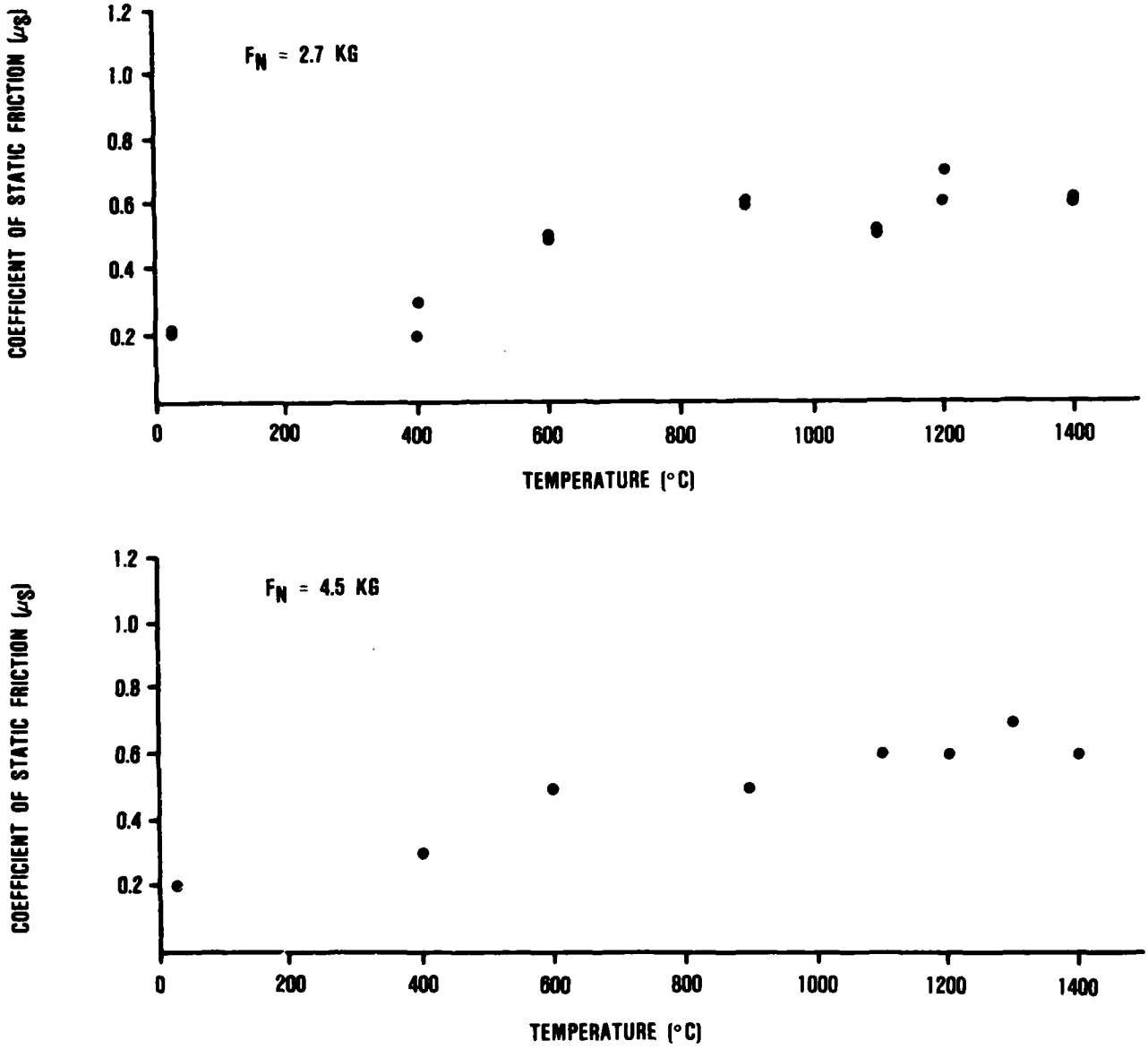

Figure 15. Coefficient of Static Friction as a Function of Temperature for CSZ at Normal Forces of 2.7 and 4.5 kg (Line Contact, 0.05 cm/min Sliding Rate).

compared to values for SASC. At elevated temperatures (>900°C), there is as much as a two-fold difference in the measured μ_S. The coefficients of friction for CSZ are approximately 0.18 at room temperature, increase to approximately 0.5 at 600°C, and then remain approximately constant (0.5 to 0.7) up to 1400°C. The dramatic differences in behavior between the SASC and CSZ specimens further support the viscous layer hypothesis to explain the elevated-temperature contact behavior of SASC.

As shown in Figure 13, the F_R measured for CSZ is small. There is no clear trend as to the effect of temperature on F_R, but F_R does increase with normal forces (Table 2). The magnitude, negligible temperature effect, and normal force effects would be consistent with a purely elastic behavior.

Figure 16 presents scanning electron photomicrographs of typical contact areas for SASC and CSZ specimens after testing at 1300°C with a 2.7 kg normal force. There is negligible evidence of contact on the CSZ compared to the SASC.

Figure 17 presents scanning electron photomicrographs of typical contact areas for CSZ specimens after testing at room temperature, 900°, 1200°, and 1400°C. There is no evidence of a glassy layer over the temperature range studied. In fact, the figure shows the microstructure of the specimen, with no apparent surface layer. .

The room-temperature retained strength after contact testing was measured (Table 3) and compared to the baseline room-temperature strength (Table 4). None of the retained-strength specimens failed in the contact area. Because of the limited data, however, no significance can be placed on the difference between the retained strength and the baseline value. It is concluded that, at the normal forces applied in this investigation, CSZ does not exhibit contact damage.

TABLE 2. RESULTS FOR LINE-CONTACT TESTING OF ZDY4 CSZ ON ZDY4, 0.05 CM/MIN SLIDING RATE.

Temperature (°C)	F_S (kg)	μ_S	F_D (kg)	μ_D	F_R (kg)
F_N = 0.5 kg					
Room Temp	0.09	0.2	0.09	0.2	0.00
400	0.09	0.2	0.14	0.3	0.00
600	0.23	0.5	0.27	0.6	0.05
900	0.31	0.7	0.54	1.2	0.05
1100	0.13	0.3	0.18	0.4	0.05
1200	0.18	0.4	0.27	0.6	0.00
1300	0.31	0.7	0.27	0.6	0.05
1400	0.23	0.5	0.27	0.6	0.00
F_N = 1.4 kg					
Room Temp	0.18	0.1	0.18	0.1	0.05
400	0.27	0.2	0.50	0.4	0.05
600	0.73	0.5	0.68	0.5	0.05
900	0.73	0.5	1.00	0.7	0.10
1100	0.63	0.5	0.77	0.6	0.10
1200	0.77	0.6	0.91	0.7	0.00
1300	0.86	0.6	0.82	0.6	0.05
1400	0.77	0.6	0.73	0.5	0.10
F_N = 2.7 kg					
Room Temp	0.45	0.2	0.36	0.1	0.05
Room Temp	0.45	0.2	0.41	0.2	0.05
400	0.63	0.2	0.68	0.3	0.10
400	0.86	0.3	0.68	0.3	0.05
600	1.22	0.5	1.36	0.5	0.05
600	1.22	0.5	1.50	0.6	0.10
900	1.63	0.6	1.91	0.7	0.10
900	1.63	0.6	1.86	0.7	0.20
1100	1.27	0.5	1.41	0.5	0.05
1100	1.22	0.5	1.50	0.6	0.00
1200	1.90	0.7	2.09	0.8	0.20
1200	1.63	0.6	1.54	0.6	0.00
1300	1.77	0.7	1.63	0.6	0.10
1300	1.77	0.7	1.54	0.6	0.10
1400	1.54	0.6	1.50	0.6	0.10
1400	1.54	0.6	1.63	0.6	0.20

TABLE 2. RESULTS FOR LINE-CONTACT TESTING OF ZDY4 CSZ ON ZDY4, 0.05 CM/MIN SLIDING RATE (CONT'D).

Temperature (°C)	F_S (kg)	μ_S	F_D (kg)	μ_D	F_R (kg)
F_N = 4.5 kg					
Room Temp	0.81	0.2	0.63	0.1	0.10
400	1.13	0.3	1.13	0.3	0.10
600	2.36	0.5	2.63	0.6	0.10
900	2.36	0.5	3.08	0.7	0.30
1100	2.72	0.6	2.50	0.6	0.20
1200	2.50	0.6	2.68	0.6	0.10
1300	3.04	0.7	2.63	0.6	0.20
1400	2.86	0.6	2.54	0.6	0.30

(A) SASC

(B) CSZ

Figure 16. Scanning Electron Photomicrographs of SASC and CSZ Contact Areas after Testing at 1300°C and a 2.7 kg Normal Force.

MP-89731

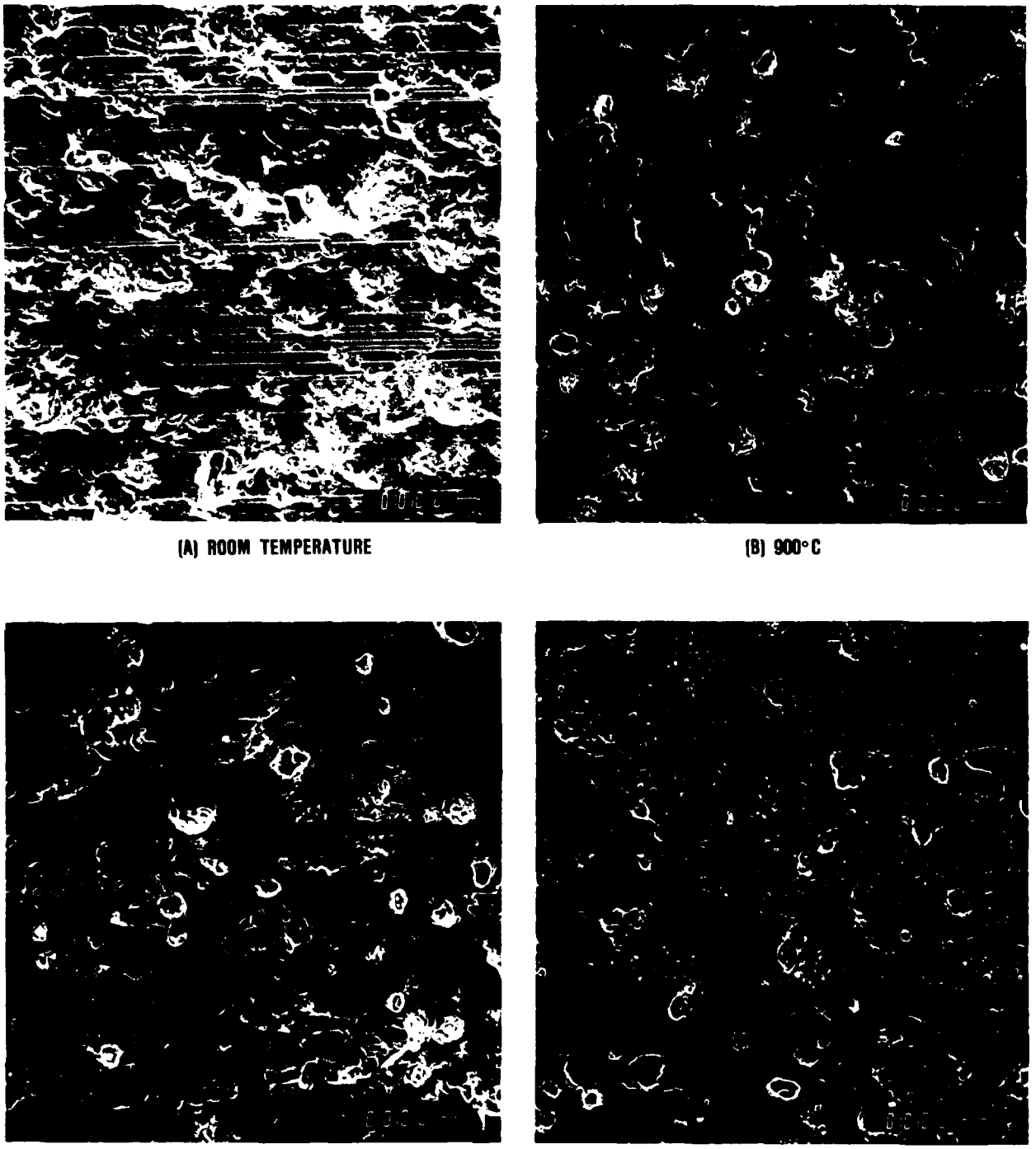

Figure 17. Scanning Electron Photomicrographs of CSZ Contact Areas after Testing at Various Temperatures and a 2.7 kg Normal Force.

TABLE 3. ROOM-TEMPERATURE RETAINED STRENGTH OF CSZ.

Test Temperature (°C)	Retained Strength[1] (ksi)	Fracture Origin[2]	Fracture in Contact Area
Normal Force = 1.4 kg			
Room Temp	28.9	Tensile Face	No
400	25.1	Tensile Face	No
600	28.2	Tensile Face	No
900	-	-	-
1100	23.4	Surface Pore	No
1200	24.1	Tensile Face	No
1300	20.6	Chamfer	No
1400	24.1	Tensile Face	No
Normal Force = 2.7 kg			
Room Temp	28.9	Tensile Face	No
400	28.2	Tensile Face	No
600	26.5	Tensile Face	No
900	25.8	Tensile Face	No
1100	17.5	Tensile Face	No
1200	23.0	Tensile Face	No
1300	24.4	Tensile Face	No
1400	26.1	Tensile Face	No
Normal Force = 4.5 kg			
Room Temp	26.8	Tensile Face	No
400	22.7	Chamfer	No
600	27.9	Tensile Face	No
900	25.1	Tensile Face	No
1100	24.1	Tensile Face	No
1200	24.4	Tensile Face	No
1300	23.4	Tensile Face	No
1400	25.1	Tensile Face	No

[1] Quarter-point bend, 1.5-inch outer span, 0.75-inch inner span

[2] Optical microscopy, 40X

TABLE 4. ROOM-TEMPERATURE BASELINE STRENGTH OF CSZ.

Specimen No.	Flexure Strength[1] (ksi)	Fracture Origin[2]
12716	31.6	Tensile Face
12717	29.9	Missing
12718	28.8	Tensile Face
12719	26.5	Tensile Face
12720	31.7	Tensile Face
12721	29.2	Tensile Face
12722	32.8	Tensile Face
12723	25.5	Chamfer
12724	32.2	Tensile Face
12725	30.9	Tensile Face
Average	29.9	

1 Quarter-point bend, 1.5-inch outer span, 0.75-inch inner span

2 Optical microscopy, 40X

6.0 CONCLUSIONS AND RECOMMENDATIONS

Work accomplished during this reporting period leads to the following conclusions and recommendations:

- The results strongly indicate that a viscous mechanism is a major contributor to the contact behavior of Sintered Alpha SiC (SASC) at elevated temperatures.

- The coefficient of friction for SASC tends to increase with temperature up to approximately 1300°C and then decreases with increasing temperature.

- The coefficient of friction for cubic stabilized ZrO_2 (CSZ) is low over the range of room temperature to 1400°C. CSZ does not exhibit contact damage over this temperature range for normal forces up to 4.5 kg in line contact for the geometry studied.

- Additional work is required to incorporate the high-temperature contact behavior of a material in a design analysis. An analytical model must be developed that accounts for the viscous behavior of SASC at the contact interface at elevated temperatures. As a minimum, this model should include contact area, thickness and viscosity of the viscous layer, and temperature.

7.0 LIST OF REFERENCES

1. "Contact-Stress Analysis of Ceramic-to-Metal Interfaces," Final Report Contract N00014-78-C-0547, September 21, 1979. Garrett Report No. 21-3239.

2. "Contact-Stress Analysis of Ceramic-to-Metal Interfaces," Final Report Contract N00014-79-C-0867, September 2, 1980. Garrett Report No. 21-3690.

3. "Contact-Stress Analysis of Ceramic-to-Metal Interfaces," Annual Report Contract N00014-80-C-0870, October 9, 1981. Garrett Report No. 21-4140.

4. "Contact-Stress Analysis of Elastic-Viscoelastic Interface Conditions," Annual Report Contract N00014-80-C-0870, December 1982. Garrett Report No. 21-4140(1).

5. D. W. Richerson, L. J. Lindberg, and C. Dins, AiResearch Report No. 76-212188(17), "Ceramic Gas Turbine Engine Demonstration Program," Interim Report No. 17 (Quarterly), May 1980, Navy Contract N00024-76-C-5352.

6. D. W. Richerson, W. D. Carruthers, and L. J. Lindberg, "Contact Stress and Coefficient of Friction Effects on Ceramic Interfaces" in Surfaces and Interfaces in Ceramic and Ceramic-Metal Systems, J. Pask and A. Evans, eds., Plenum Press, 1981, pp. 661-676.

7. D. W. Richerson, L. J. Lindberg, W. D. Carruthers, and J. Dahn, "Contact Stress Effects on Si_3N_4 and SiC Interfaces," Ceramic Engineering and Science Proceedings, 2 [7-8], 1981.

8. J. R. Smyth and D. W. Richerson, "High-Temperature Dynamic-Contact Behavior of Sintered Alpha Silicon Carbide," Ceramic Engineering and Science Proceedings, 4 [7-8], 1983.

9. "High-Temperature Ceramic Interface Study," Semi-Annual Progress Report NASA Contract DEN3-324, September 19, 1983. Garrett Report No. 31-4973(06).

8.0 LIST OF REPORTS/PUBLICATIONS

The following reports/publications have been presented during the period of this contract:

- "Contact-Stress Analysis of Ceramic-to-Metal Interfaces," Annual Report Contract N00014-80-C-0870, October 9, 1981. Garrett Report No. 21-4140.

- "Contact-Stress Analysis of Elastic-Viscoelastic Interface Conditions," Annual Report for Contract N00014-80-C-0870, December 1982, Garrett Report No. 21-4140(1).

- J. R. Smyth and D. W. Richerson, "High-Temperature Dynamic-Contact Behavior of Sintered Alpha Silicon Carbide," Ceramic Engineering and Science Proceedings, 4 [7-8], 1983.

- End-of-the-Year Letter Reports on Contract N00014-80-C-0870, 1981, 1982, 1983.

- D. W. Richerson, D. G. Finger, and J. M. Wimmer, "Analytical and Experimental Evaluation of Biaxial Contact Stress," Fracture Mechanics of Ceramics, 5, 1983.

- D. W. Richerson, "Contact Stresses at Ceramic Interfaces," Nitrogen Ceramics II, 1982.

END

FILMED

4-84

DTIC